ACS APPLIED MATERIALS & INTERFACES

Research Article

www.acsami.org

Design of Polypyrrole/Polyaniline Double-Walled Nanotube Arrays for Electrochemical Energy Storage

Zi-Long Wang, Xu-Jun He, Sheng-Hua Ye, Ye-Xiang Tong, and Gao-Ren Li*

MOE Laboratory of Bioinorganic and Synthetic Chemistry, KLGHEI of Environment and Energy Chemistry, School of Chemistry and Chemical Engineering, Sun Yat-sen University, Guangzhou 510275, China

ABSTRACT: The novel hybrid polypyrrole (PPy)/polyaniline (PANI) double-walled nanotube arrays (DNTAs) were designed to exploit the synergistic effects and shape effects for supercapacitive energy storage. The PPy/PANI DNTAs showed large specific capacitance (C_{sp}) of 693 F/g at a scan rate of 5 mV/s. The PPy/PANI DNTAs also exhibited good rate capability and high long-term cycle stability (less 8% loss of the maximum specific capacitance after 1000 cycles). The synergistic effects between PPy and PANI, the shape effects of nanotube arrays and double-walled nanostructures, and high utilization rate of electrode are crucial for the outstanding performance of PPy/PANI DNTAs. The large C_{sp}, good rate capability, and high long-term cycle stability offered by the PPy/PANI DNTAs, make them promising candidate electrodes for high-performance supercapacitors.

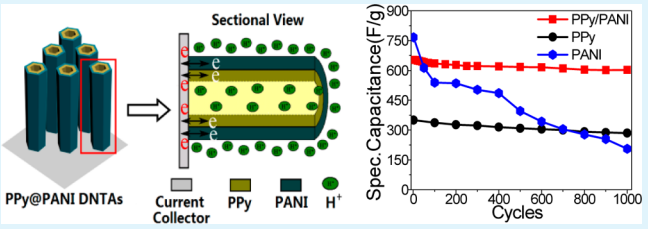

KEYWORDS: *polypyrrole, polyaniline, double-walled nanotube, supercapacitor*

1. INTRODUCTION

Supercapacitors, as a new class of energy-storage and power-supply devices, are developed to meet the increasing demand for applications in powering vehicles and portable electronic devices because of their high power density, long cycle-life, simple principle, and speedy dynamic of charge propagation.[1] To date, various materials, including carbonaceous materials,[2] conducting polymers,[3−7] and transition-metal oxides/hydroxides,[8−11] have been extensively studied as electrodes for supercapacitors. However, the electrode composed of above single material usually can not fulfill the requirements of future electrical energy storage devices because of the inherent material limitations such as low energy density, slow kinetics (low power density), or weak mechanical stability. Recently, the hybrid electrode materials have attracted great attention for energy storage because of the combining unique properties of individual materials with synergistic effects, realizing the full potential of electrode materials in terms of performance (e.g. excellent mechanical stability, high energy density, and high power density).[12−15]

The designs of hybrid electrode materials have been widely investigated, and most of them focused on pseudocapacitive material/conductive matrix hybrid materials, such as NiO/Ni,[16] MnO_2/SnO_2,[17] MnO_2/Zn_2SnO_4,[18] MnO_2/graphene,[19] and polyaniline/graphene.[20,21] When the unique properties of individual constituents are combined, it has been demonstrated that the performance of such an electrode can be improved. In the above cases, the pseudocapacitive materials are relatively low weight fractions in electrodes and usually have excellent rate and cycling performance. However, the energy and power densities of electrode are often sacrificed, and this prevents the supercapacitors from becoming primary power supplies that are commercially viable. To overcome the above shortcomings, some efforts have been devoted to searching for hybrid pseudocapacitive materials such as the mixed metal oxides, binary metal oxide/hydroxides, and mixed conducting polymers.[22] However, the pseudocapacitive performance of this kind of hybrid materials usually is not satisfactory because of lack of well-defined nanostructures and good synergistic effects. A pivotal challenge in this field is to construct an integrated smart nanoarchitecture for hybrid pseudocapacitive materials with excellent synergistic effects,[23,24] in which the structural feature and electroactivity of every component can be fully manifested and rapid ion and electron transports can be provided.

Herein, the novel polypyrrole (PPy)/polyaniline (PANI) double-walled nanotube arrays (DNTAs) are designed to exploit the synergistic effects and shape effects for electrochemical energy storage. The PANI and PPy both are promising pseudocapacitive materials because of their good electrical conductivity, high energy storage capacity, environment-friendness, and low-cost synthesis,[25−28] and they have the unique complemental performance and can co-contribute to the enhancement of pseudocapacitive performance of electrode. The orderly aligned DNTAs represent a novel prime example of materials with well-defined pore structures because of the uniquely hollow structures, double-walled structures, array structures, and anisotropic nature. It has been demonstrated that the diffusion parallel to nanotube array orientation can be exceedingly fast, achieving nearly the same speed as ion

Received: October 27, 2013
Accepted: December 6, 2013
Published: December 6, 2013

 © 2013 American Chemical Society

Scheme 1. Schematic Illustration for the Fabrication of PPy/PANI DNTAs

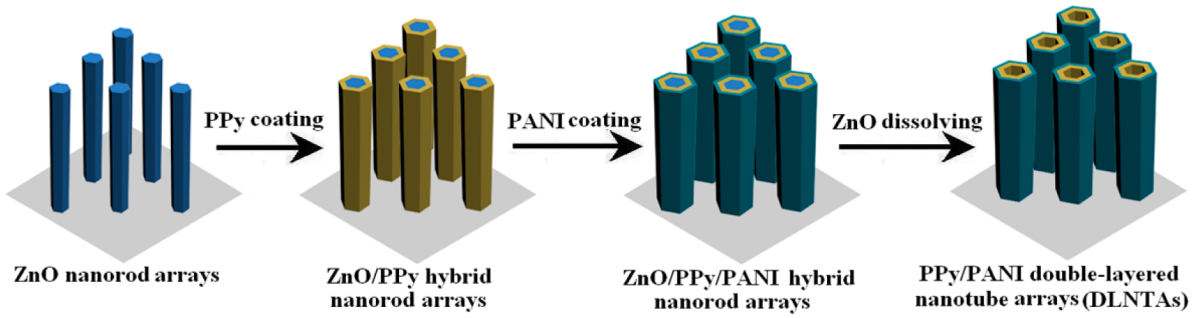

diffusion in a bulk electrolyte and substantially reducing resistance of electrolyte penetration/diffusion.[29] In addition, the DNTAs can provide large surface area, high utilization rate, and sufficient mass loading to store sufficient energy. What's more important is that the outer layer in DNTAs does not prohibit ion permeation into the inner layer because of the hollow nanotube array. Therefore, the PPy/PANI DNTAs are hoped to have superior pseudocapacitive performance because of the above favorable characteristics.

ZnO nanorod array template-assisted electrodeposition method is developed for the synthesis of novel PPy/PANI DNTAs. The utilized template electrodeposition route shows following merits: (i) the hybrid PPy/PANI DNTAs can be easily synthesized, (ii) the orderly DNTAs can directly grow on current collector in a good solid contact, which largely enhances the conductivity, (iii) the conducting additives and binders are not needed for the fabrication of electrode because of the good solid contact between current collector and PPy/PANI DNTAs, and accordingly the weight and volume of electrode will be reduced. Electrochemical measurements show the synthesized PPy/PANI DNTAs exhibit high specific capacitance (C_{sp}), good rate capability, and excellent long-term cycle stability because of the compositional (i.e., PPy/PANI) and geometrical (i.e., DNTA structure) properties of materials, and are promising electrode materials for the next-generation high-performance supercapacitors.

2. EXPERIMENTAL SECTION

ZnO nanorod arrays (NRAs) as templates were electrodeposited in a solution of 0.01 M $Zn(NO_3)_2$ +0.05 M NH_4NO_3 by galvanostatic electrolysis at a current density of 1.0 mA cm^{-2} for 90 min at 70 °C using HDV-7C transistor potentiostatic apparatus on a Ti substrate (1.0 cm^2). Then the electro-deposition of PPy was carried out on the surfaces of ZnO NRAs in a solution of 0.01 M pyrrole + 0.05 M Na_2SO_4 by galvanostatic electrolysis at a current density of 1.0 mA cm^{-2} for 20 min at 70 °C using DJS-292B transistor potentiostatic apparatus. After that, PANI layers were further electrode-posited on the surf-aces of ZnO/PPy NRAs in a solution of 0.1 M aniline +0.05 M Na_2SO_4 by galv-anostatic electrolysis at a current density of 1.0 mA cm^{-2} for 30 min at 70 °C using HDV-7C transistor potentiostatic apparatus. At last, the synthesized ZnO/PPy/PANI NRAs were put into 28% ammonia water for 2 h to remove ZnO, and accordingly PPy/PANI DNTAs were synthesized. The surface morphologies and microstructures of the prepared samples were examined by using field-emission environment scanning electron microscope (SEM, FEI, Quanta 400) and transmission electron microscopy (TEM, JEOL JEM-2010HR). The structures of the prepared hybrid materials were analyzed by X-ray diffraction (XRD, PIGAKU, D/MAX 2200 VPC). Optical properties of PPy/PANI DNTAs were tested by Fourier transform infrared spectrum (FT-IR, Nicolet 330) and Raman spectrometer (Renishawin Via).

The electrochemical properties of the synthesized PPy/PANI DNTAs were studied in a CHI760D electrochemical workstation by cyclic voltammetry in a three-electrode cell at room temperature. A graphite sheet was used as the counter electrode. A saturated calomel electrode (SCE) was used as the reference electrode. The hybrid nanotube arrays were used as the working electrode. The cyclic voltammetry experiments were performed in 1.0 M H_2SO_4 solution at a scan rate of 5−250 mV/s.

3. RESULTS AND DISCUSSION

The procedure used to synthesize PPy/PANI DNTAs is shown in Scheme 1, and it is described in the Experimental Section. SEM images of the synthesized ZnO NRAs template, ZnO/PPy NRAs, and ZnO/PPy/PANI NRAs are shown in Figure 1a, 1b, and 1c, respectively. Compared with ZnO NRAs template, PPy layers are clearly seen on ZnO NRAs as shown in Figure 1b.

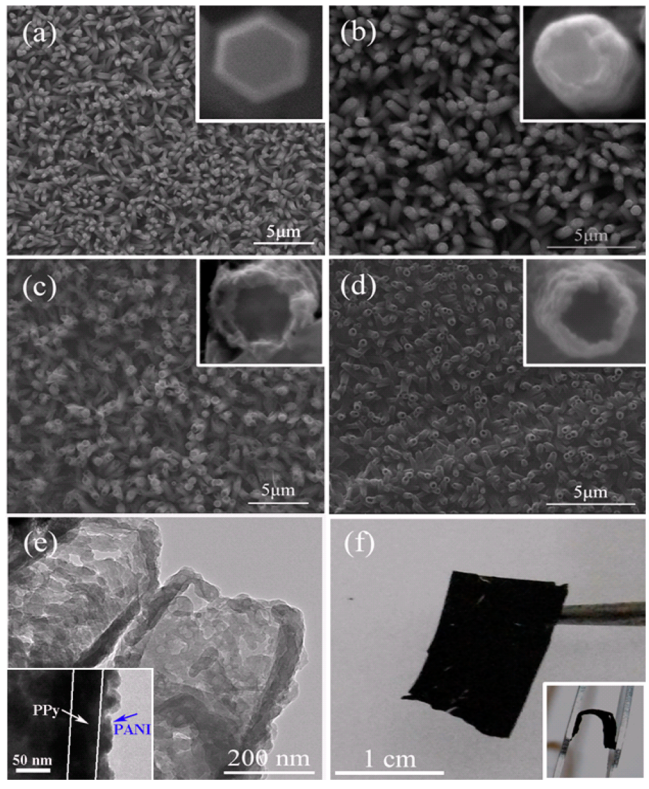

Figure 1. SEM images of (a) ZnO NRAs template, (b) ZnO/PPy NRAs, (c) ZnO/PPy/PANI NRAs, and (d) PPy/PANI DNTAs. (e) TEM image of the typical PPy/PANI DNTAs. (f) Optical image of PPy/PANI DNTAs film in a large-scale area. (Inset in f is optical image of PPy/PANI DNTAs film under the slight bending).

dx.doi.org/10.1021/am404751k | ACS Appl. Mater. Interfaces 2014, 6, 642−647

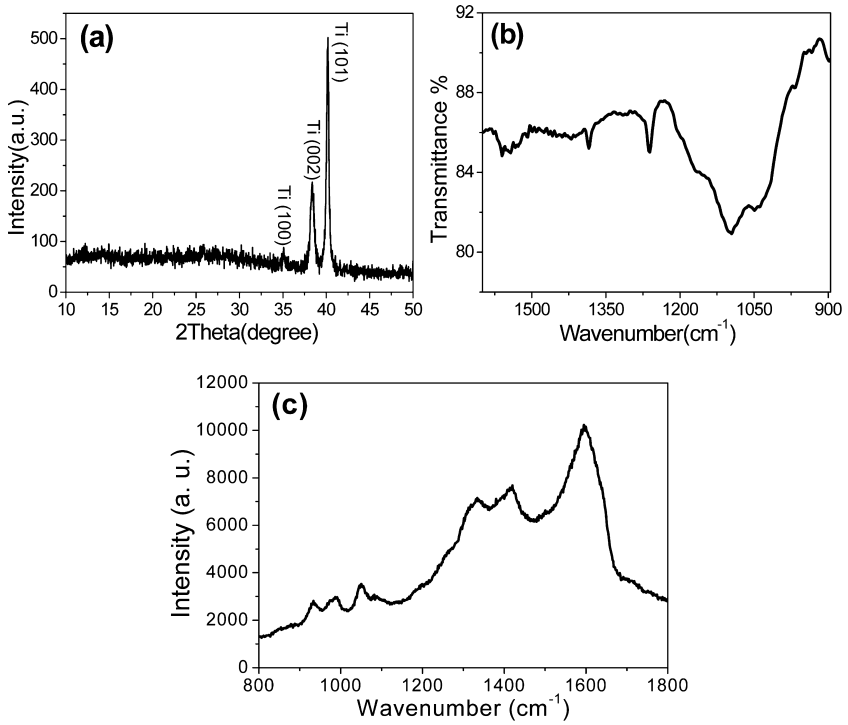

Figure 2. (a) XRD, (b) FT-IR, and (c) Raman spectra of PPy/PANI DNTAs.

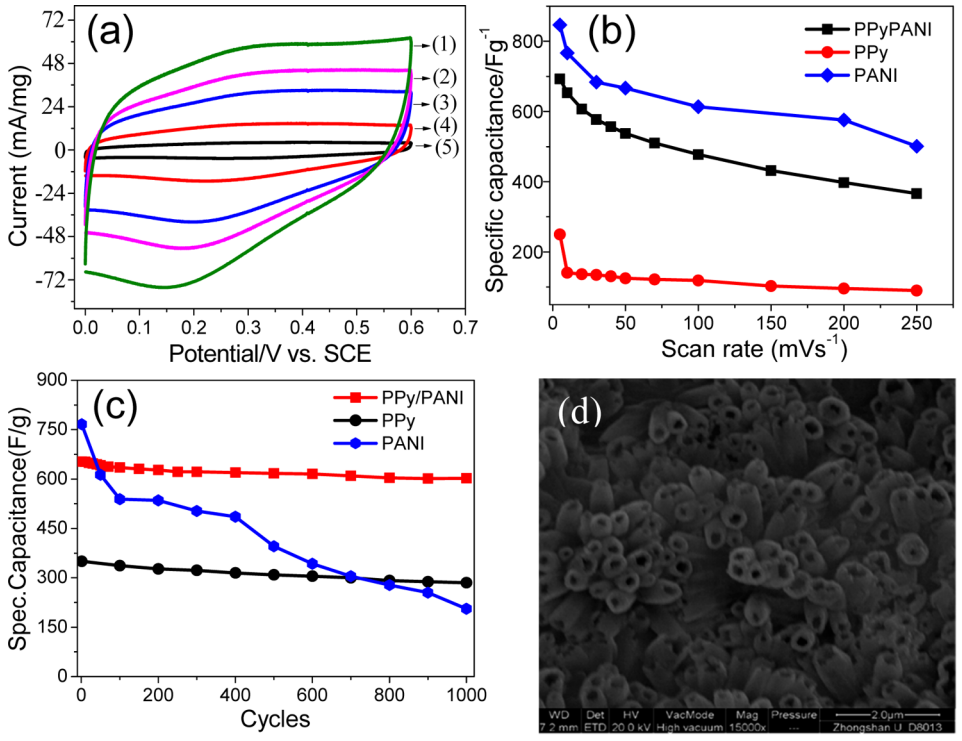

Figure 3. (a) CVs of PPy/PANI DNTAs at different scan rates: (1) 100 mV s^{-1}, (2) 70 mV s^{-1}, (3) 50 mV s^{-1}, (4) 20 mV s^{-1}, (5) 5 mV s^{-1}; (b) C_{sp} values of PPy/PANI DNTAs, PPy nanotube arrays and PANI nanotube arrays as a function of scan rate; (c) C_{sp} values of PPy/PANI DNTAs, PPy nanotube arrays and PANI nanotube arrays as a function of cycle number at 10 mV s^{-1}; (d) SEM image of PPy/PANI DNTAs after 1000 cycles.

Compared with ZnO/PPy NRAs, PANI layers are also clearly seen on ZnO/PPy NRAs as shown in Figure 1c. Finally, the PPy/PANI DNTAs are successfully fabricated by etching ZnO from the ZnO/PPy/PANI NRAs, and their SEM image is shown in Figure 1d. The lengths of PPy/PANI DNTAs are about 2 μm, the inner diameters are 280 nm, and the wall thicknesses are 60 nm. Figure 1e shows a typical TEM image of PPy/PANI DNTAs. The thickness of outer PANI layer is 20 nm, and that of inner PPy layer is 40 nm as shown in Figure 1e. Figure 1f shows the PPy/PANI DNTAs are easily synthesized in a large-scale area and they are flexible as shown in the inset in Figure 1f.

dx.doi.org/10.1021/am404751k | ACS Appl. Mater. Interfaces 2014, 6, 642−647

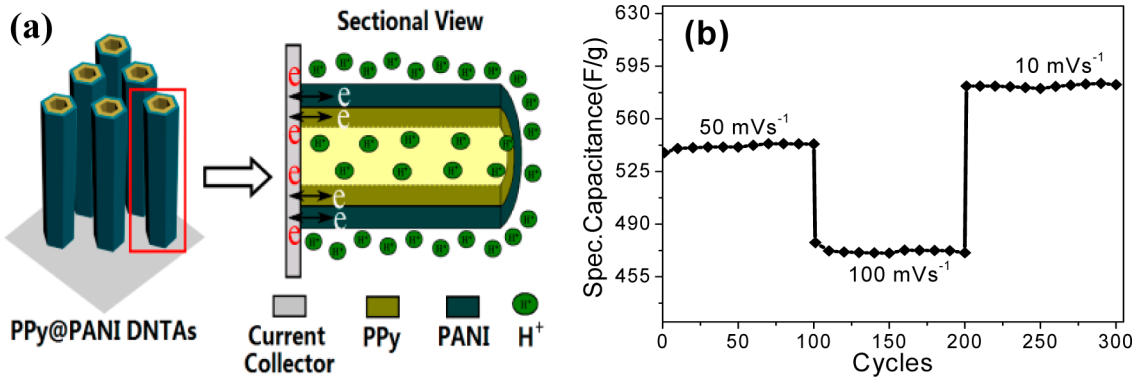

Figure 4. (a) Nanotube array architecture, double-walled structure, and high conductivity in electrode provide ion and electron "highways" and high utilization rate of electrode; (b) cycling stability of PPy/PANI DNTAs at progressively varied scan rates.

XRD pattern of the synthesized PPy/PANI DNTAs is shown in Figure 2a. Only the peaks of Ti substrate can be observed. This suggests that the PPy/PANI DNTAs are amorphous. Figure 2b shows the FT-IR spectrum of PPy/PANI DNTAs. The bands at 1560 and 1380 cm^{-1} are due to quinone-like structure and symmetric and antisymmetric ring-stretching modes of PANI.[30] The band at 1263 cm^{-1} is assigned to C−N stretching of a secondary aromatic amine which belongs to PANI.[31] The C−N stretching vibration of PANI appears at 1100 cm^{-1}. In addition, it is clearly seen that the characteristic peaks of polypyrrole locate at 1560 and 1480 cm^{-1}, because of the symmetric and antisymmetric ring-stretching modes, respectively.[32] The peaks at 1050 and 1315 cm^{-1} are attributed to C−H deformation vibrations and C−N stretching vibrations, respectively.[33] Raman spectrum of PPy/PANI DNTAs is shown in Figure 2c. The peaks at 1592 and 1330 cm^{-1} come from π conjugated structure and ring stretching mode of the PPy backbone, respectively. The peak at 1050 cm^{-1} corresponds to the C−H in-plane deformation of PPy. And the two small peaks at around 930 and 988 cm^{-1} are thought to be the quinoidpolaronic and bipolaronic structure of PPy, respectively.[34] The C−C stretching vibration of quinoid rings of PANI locates at 1420 cm^{-1}, and the stretching vibration of benzenoid rings of PANI appears at 1592 cm^{-1}.[35] The above results demonstrate the existences of PPy and PANI in products.

The PPy/PANI DNTAs were investigated as electrodes for supercapacitor application. Cyclic voltammograms (CVs) of the PPy/PANI DNTAs in 1.0 M H_2SO_4 electrolyte at different scan rates are shown in Figure 3a, which shows nearly rectangular shape in all CV curves, indicating symme-tric current-potential characteristics and good supercapacitive properties of PPy/PANI DNTAs. The specific capacitance (C_{sp}) of PPy/PANI DNTAs at 5 mV/s is calculated 693 F/g, which is much larger than 250 F/g of PPy nanotube arrays (NTAs) and those reported for PPy samples at the same scan rate,[36] and is close to 846 F/g of PANI NTAs that have a high theoretical C_{sp}. The dependence of C_{sp} on scan rate is shown in Figure 3b, which shows a decay of 47% in C_{sp} of PPy/PANI DNTAs with scan rate increasing from 5 to 250 mV/s. Even at a scan rate as high as 250 mV/s, the PPy/PANI DNTAs still achive a C_{sp} as large as 366 F/g. However, for PPy NTAs, the C_{sp} shows a severe decay of 64% with scan rate increasing from 5 to 250 mV/s, and it is only 90 F/g at 250 mV/s. The PPy/PANI DNTAs show much larger C_{sp} at all scan rates and much better rate capability than PPy NTAs as shown in Figure 3b and have a similar C_{sp} decay to PANI NTAs with scan rate increasing from 5 to 250 mV/s.

As we all know, besides high C_{sp}, the excellent long-term cycle stability is crucial for real super-capacitor operations. The variations of C_{sp} of PPy/PANI DNTAs, PPy NTAs, and PANI NTAs as a function of cycle number are shown in Figure 3c. As revealed from the above data, the PPy/PANI DNTAs almost can withstand over 1000 cycles without any significant decrease in C_{sp} value. It is seen that there is only a small decrease of 7.6% in C_{sp} up to 1000 cycles. In addition, the electrolyte solution still remains transparent after 1000 cycle tests, indicating almost no dissolution of PPy/PANI DNTAs into solution. However, the PANI NTAs show much more severe C_{sp} decay than PPy/PANI DNTAs after 1000 cycles as shown in Figure 3c. The C_{sp} decrease of PANI NTAs is about 73.1% after 1000 cycles, indicating that the individual PANI NTAs are not ideal candidates for supercapacitor applications although they have high C_{sp} in initial stage. For PPy NTAs, the decrease of C_{sp} is about 18.6% after 1000 cycles, which is also more severe than that of PPy/PANI DNTAs. The above results demonstrate PPy/PANI DNTAs synchronously own large C_{sp} and excellent long-term cycle stability, and they are much superior to individual PPy NTAs and PANI NTAs for supercapacitor applications.

The combination of PPy and PANI with independent electroactivities into DNTAs architecture observably improve the electrochemical performance, especially the cycle stability, compared with the individual PANI and PPy NTAs. The above situation is different from the performance enhan-cements by the previous core-shell structures, such as MnO_2/ZnO,[37] MoO_3/ZnO,[38] and MnO_2/Mn,[39] in which only the shell materials acted as active materials while the core materials were only current collectors. Here it is believed that the synergistic effects from hybrid pseudocapacitive PANI and PPy materials and the shape effects of ordered DNTA configurations have important contribution to high C_{sp}, excellent long-term cycle stability, and high rate capability of PPy/PANI DNTAs. The composites of PPy and PANI have the unique complemental performance compared with individual PANI and PPy and the following synergistic effects have been demonstrated: (i) PPy/PANI DNTAs show excellent long-term cycle stability and can overcome the weak point of PANI NTAs that have poor cycle stability (Figure 3c). After 1000 cycles, the surface morphology of PPy/PANI DNTAs still is kept well as shown in Figure 3d. (ii) the combination of PPy and PANI leads to PPy/PANI DNTAs have much higher C_{sp} and rate capability than PPy

dx.doi.org/10.1021/am404751k | ACS Appl. Mater. Interfaces 2014, 6, 642−647

NTAs, overcoming the weak points of PPy NTAs that have low C_{sp} and rate capability. The above improvements may be attributed to the synergistic effects produced by the favorable interactions between PPy and PANI layers at the interfaces. In addition, the PPy/PANI DNTAs have smart shape effects and show following advantages as super-capacitor electrode: (i) The PPy/PANI DNTAs will relax the transport of ions because of hollow nanostructures as shown in Figure 4a.[39] Also, the double thin layers of PPy and PANI in DNTAs will enable fast, reversible faradic reactions and provide short ion diffusion paths. (ii) The DNTAs with double PPy and PANI shells can obviously enhance the utilization rate of electrode materials because of the anisotropic morphologies, large specific surface areas, and hollow nanostructures. (iii) The DNTAs directly grow on conductive substrate have excellent electrical contacts with current collec-tor (Figure 4a), and this will let each PPy/PANI nanotube effectively participate in electrochemical reactions and almost no "dead" volume. Therefore, the above synergistic effects and shape effects between PPy and PANI jointly promote the synthesized PPy/PANI composites to have high C_{sp}, excellent long-term cycle stability, and high rate capability.

To further investigate the advantage of PPy/PANI DNTAs, we tested their cycle performance at progressively increased scan rate, and the results are recorded in Figure 4b. Here even we find the electrode material suffered from sudden scan rate change, the PPy/PANI DNTAs still show the stable C_{sp} at each scan rate. What is more important is that the C_{sp} can still keep 470 F/g when the scan rate increases to 100 mV/s. The above results further demonstrate that the synthesized PPy/PANI DNTAs could meet the requirements of both long cycle lifetime and good rate capability, which are highly important for utilization in the practical energy storage devices.

4. CONCLUSIONS

In summary, the novel hybrid PPy/PANI DNTAs were designed and fabricated to exploit the synergistic effects and shape effects for electrochemical energy storage. The preliminary studies indicate that the PPy/PANI DNTAs have high C_{sp}, excellent rate capability and superior long-term cycle stabilitys. The synergistic effects together with shape effects of PPy and PANI are responsible for the prominently enhanced electrochemical performance of PPy/PANI DNTAs. Here the reported electrode design concept also can be used for inorganic materials, such as MnO_2, NiO, and Co_3O_4, to build the multifunctional hybrid nano-/microstructures, which will be promising for a large spectrum of nanodevice applications.

AUTHOR INFORMATION

Corresponding Author

*E-mail: ligaoren@mail.sysu.edu.cn. Tel.: +86 20 84110081. Fax: +86 20 84110081.

Notes

The authors declare no competing financial interest.

ACKNOWLEDGMENTS

This work was supported by NSFC (51173212 and 21073240), Natural Science Foundation of Guangdong Province (S2013020012833), Fundamental Research Fund for the Central Universities (13lgpy51), Fund of New Star Scientist of Pearl River Science and Technology of Guangzhou (2011J2200057), SRF for ROCS, SEM ([2012]1707), and Open-End Fund of State Key Lab of Physical Chemistry of Solid Surfaces of Xiamen University (201113).

REFERENCES

(1) Lu, X.; Zhai, T.; Zhang, X.; Shen, Y.; Yuan, L.; Hu, B.; Gong, L.; Chen, J.; Gao, Y.; Zhou, J.; Tong, Y.; Wang, Z. L. *Adv. Mater.* **2012**, *24*, 938−944.
(2) Zhai, Y.; Dou, Y.; Zhao, D.; Fulvio, P.; Mayes, R.; Dai, S. *Adv. Mater.* **2011**, *23*, 4828−4850.
(3) Liu, R.; Duay, J.; Lee, S. B. *ACS Nano* **2010**, *4*, 4299−4307.
(4) Ghosh, S.; Inganas, O. *Adv. Mater.* **1999**, *11*, 1214−1218.
(5) Kumar, N. A.; Choi, H.-J.; Shin, Y. R.; Chang, D. W.; Dai, L.; Baek, J.-B. *ACS Nano* **2012**, *6*, 1715−1723.
(6) Meng, C.; Liu, C.; Chen, L.; Hu, C.; Fan, S. *Nano Lett.* **2010**, *10*, 4025−4030.
(7) Cho, S. I.; Lee, S. B. *Acc. Chem. Res.* **2008**, *41*, 699−707.
(8) Wei, T.-Y.; Chen, C.-H.; Chien, H.-C.; Lu, S.-Y.; Hu, C.-C. *Adv. Mater.* **2010**, *22*, 347−351.
(9) Brezesinski, T.; Wang, J.; Tolbert, S.; Dunn, B. *Nature Mater* **2010**, *9*, 145−149.
(10) Rakhi, R. B.; Chen, W.; Cha, D.; Alshareef, H. N. *Nano Lett.* **2012**, *12*, 2559−2567.
(11) Chen, W.; Rakhi, R. B.; Hu, L.; Xie, X.; Cui, Y.; Alshareef, H. N. *Nano Lett.* **2011**, *11*, 5165−5172.
(12) Chen, Z.; Augustyn, V.; Wen, J.; Zhang, Y.; Shen, M.; Dunn, B.; Lu, Y. *Adv. Mater.* **2011**, *23*, 791−795.
(13) Liu, C.; Li, F.; Ma, L.-P.; Cheng, H.-M. *Adv. Mater.* **2010**, *22*, E28−E62.
(14) Kim, J.-H.; Zhu, K.; Yan, Y.; Perkins, C. L.; Frank, A. J. *Nano Lett.* **2010**, *10*, 4099−4104.
(15) Xia, X.; Tu, J.; Zhang, Y.; Wang, X.; Gu, C.; Zhao, X.-B.; Fan, H. J. *ACS Nano* **2012**, *6*, 531−5538.
(16) Lu, Q.; Lattanzi, M. W.; Chen, Y.; Kou, X.; Li, W.; Fan, X.; Unruh, K. M.; Chen, J.; Xiao, J. Q. *Angew. Chem. Int. Ed.* **2011**, *50*, 6847−6850.
(17) Yan, J.; Khoo, E.; Sumboja, A.; Lee, P. S. *ACS Nano* **2010**, *4*, 4247−4255.
(18) Bao, L.; Zang, J.; Li, X. *Nano Lett.* **2011**, *11*, 1215−1220.
(19) Yu, G.; Hu, L.; Liu, N.; Wang, H.; Vosgu-eritchian, M.; Yang, Y.; Cui, Y.; Bao, Z. *Nano Lett.* **2011**, *11*, 4438−4442.
(20) Xu, J.; Wang, K.; Zu, S.-Z.; Han, B.-H.; Wei, Z. *ACS Nano* **2010**, *4*, 5019−5026.
(21) Wu, Q.; Xu, Y.; Yao, Z.; Liu, A.; Shi, G. *ACS Nano* **2010**, *4*, 1963−1970.
(22) Guan, C.; Li, X.; Wang, Z.; Cao, X.; Soci, C.; Zhang, H.; Fan, H. J. *Adv. Mater.* **2012**, *24*, 4186−4190.
(23) Liu, J.; Jiang, J.; Cheng, C.; Li, H.; Zhang, J.; Gong, H.; Fan, H. J. *Adv. Mater.* **2011**, *23*, 2076−2081.
(24) Mai, L.-Q.; Yang, F.; Zhao, Y.-L.; Xu, X.; Xu, L.; Luo, Y. *Nature Commun.* **2011**, *2*, 381−383.
(25) Zhang, L. L.; Li, S.; Zhang, J.; Guo, P.; Zheng, J.; Zhao, X. S. *Chem. Mater.* **2010**, *22*, 1195−1202.
(26) Li, C.; Bai, H.; Shi, G. *Chem. Soc. Rev.* **2009**, *38*, 2397−2409.
(27) Tran, H. D.; Li, D.; Kaner, R. B. *Adv. Mater.* **2009**, *21*, 1487−1499.
(28) Wang, D.-W.; Li, F.; Zhao, J.; Ren, W.; Chen, Z.-G.; Tan, J.; Wu, Z.-S.; Gentle, I.; Lu, G. Q.; Cheng, H.-M. *ACS Nano* **2009**, *3*, 1745−1752.
(29) Izadi-Najafabadi, A.; Futaba, D. N.; Iijima, S.; Hata, K. *J. Am. Chem. Soc.* **2010**, *132*, 18017−18019.
(30) Liu, W.; Kumar, J.; Tripathy, S.; Senecal, K.; Samuelson, L. *J. Am. Chem. Soc.* **1999**, *121*, 71−78.
(31) Li, G.-R.; Feng, Z.-P.; Zhong, J.-H.; Wang, Z.-L.; Tong, Y.-X. *Macromolecules* **2010**, *43*, 2178.
(32) Zhang, X.; Zhang, J.; Song, W. H.; Liu, Z. F. *J. Phys. Chem. B* **2006**, *110*, 1158−1165.
(33) Tian, B.; Zerbi, G. *J. Chem. Phys.* **1990**, *92*, 3886−3888.
(34) Biswas, S.; Drzal, L. T. *Chem. Mater.* **2010**, *22*, 5667−5671.

(35) Luo, C. H.; Peng, H.; Zhang, L. J.; Lu, G. L.; Wang, Y. T.; Sejdic, J. T. *Macromolecules* **2011**, *44*, 6899−6907.
(36) Liu, A.; Li, C.; Bai, H.; Shi, G. *J. Phys. Chem. C* **2010**, *114*, 22783−22789.
(37) He, Y.-B.; Li, G.-R.; Wang, Z.-L.; Su, C.-Y.; Tong, Y.-X. *Energy Environ. Sci.* **2011**, *4*, 1288−1292.
(38) Li, G.-R.; Wang, Z.-L.; Zheng, F.-L.; Ou, Y.-N.; Tong, Y.-X. *J. Mater. Chem.* **2011**, *21*, 4217−4221.
(39) Hu, C.-C.; Chang, K.-H.; Lin, M.-C.; Wu, Y.-T. *Nano Lett.* **2006**, *6*, 2690−2695.